Positron beam study of indium tin oxide films on GaN

2007 J. Phys.: Condens. Matter 19 086204

(http://iopscience.iop.org/0953-8984/19/8/086204)

IOP PUBLISHING JOURNAL OF PHYSICS: CONDENSED MATTER

J. Phys.: Condens. Matter **19** (2007) 086204 (10pp) doi:10.1088/0953-8984/19/8/086204

Positron beam study of indium tin oxide films on GaN

C K Cheung[1], R X Wang[2], C D Beling[1], A B Djurišić[1] and S Fung[1]

[1] Department of Physics, The University of Hong Kong, Pokfulam Road, Hong Kong, People's Republic of China
[2] Institute Textiles and Clothing, The Hong Kong Polytechnic University, Kowloon, Hong Kong, People's Republic of China

Received 1 December 2006, in final form 18 January 2007
Published 6 February 2007
Online at stacks.iop.org/JPhysCM/19/086204

Abstract

Variable energy Doppler broadening spectroscopy has been used to study open-volume defects formed during the fabrication of indium tin oxide (ITO) thin films grown by electron-beam evaporation on n-GaN. The films were prepared at room temperature, 200 and 300 °C without oxygen and at 200 °C under different oxygen partial pressures. The results show that at elevated growth temperatures the ITO has fewer open volume sites and grows with a more crystalline structure. High temperature growth, however, is not sufficient in itself to remove open volume defects at the ITO/GaN interface. Growth under elevated temperature and under partial pressure of oxygen is found to further reduce the vacancy type defects associated with the ITO film, thus improving the quality of the film. Oxygen partial pressures of 6×10^{-3} mbar and above are found to remove open volume defects associated with the ITO/GaN interface. The study suggests that, irrespective of growth temperature and oxygen partial pressure, there is only one type of defect in the ITO responsible for trapping positrons, which we tentatively attribute to the oxygen vacancy.

(Some figures in this article are in colour only in the electronic version)

1. Introduction

Due to its high optical transparency and electronic conductivity, indium tin oxide (ITO) is well known as a good contacting material in the fabrication of optoelectronic devices [1, 2]. ITO thin film is commonly used as a transparent conductive coating on III–V compound devices and liquid crystal display devices [3–6]. It is commonly deposited by methods such as electron-beam evaporation [7, 8] or a range of sputtering techniques [9, 10]. The deposited coating should contain a high density of charge carriers to give good conduction together with high optical transmission. The properties of ITO film are, however, strongly dependent on the fabrication conditions such as the deposition parameters and composition of the starting materials [11]. The optimization of both the optical transparency and the electrical conductivity is still a challenging problem [12]. Many reports have been published showing the strong dependence of the electrical and optical properties of ITO on various deposition

parameters [13–15]. In particular, the internal structure and surface morphology of ITO are highly dependent on the deposition temperature and the gaseous environment [16]. Oxygen incorporation during deposition can improve the optoelectronic properties of the films because oxygen is beneficial to the removal of non-transparent metallic In and facilitates the formation of In_2O_3 from In_2O_{3-x} [16]. Some optimization is required, however, since too high an oxygen pressure during deposition produces an increased ITO electrical resistivity, which results from too few oxygen vacancies being available to donate charge carriers.

The involvement of oxygen vacancies in ITO film optimization suggests that the vacancy sensitive positron annihilation technique may yield useful information. A preliminary study of ITO films grown under different oxygen partial pressures using the positron annihilation technique has been discussed previously [17]; in that work a lower ITO *S*-parameter was observed when increasing the oxygen incorporation during deposition. The aim of this work is to provide additional information on the defect structures in the ITO film and at the ITO/n-GaN interface using positron annihilation spectroscopy. The study has been carried out under different deposition temperatures and oxygen partial pressures to observe the effects on the defect distribution within the film and interface.

2. Experimental details

ITO films were prepared by electron-beam evaporation using In_2O_3:SnO_2 (9:1) as the evaporation source. The ITO was deposited on halide vapour phase epitaxy grown n-type GaN. A proximity mask was used to produce circular contacts of 3 mm diameter. The base pressure in the chamber was 5×10^{-6} Torr. The ITO film thickness was controlled to the desired thickness using a quartz crystal monitor. Two series of ITO/GaN samples were fabricated. The first set was deposited to a thickness of 100 nm under an oxygen partial pressure of 4×10^{-3} mbar with different substrate temperatures (room temperature, 200 and 300 °C). The second set was deposited with a thickness of 200 nm and a substrate temperature of 200 °C under different oxygen partial pressures (0, 4×10^{-3}, 6×10^{-3}, 8×10^{-3} mbar). The defect–depth profiles of the samples were measured using the University of Hong Kong's (HKU) positron beam facility. The basic features of this facility have been described elsewhere [18]. The positron beam diameter was ∼1 mm allowing all the positrons to impact the ITO films. Standard variable energy Doppler broadening spectroscopy (VEDBS) scans were made by increasing the implantation energy of positrons (energy range 0–20 keV) so as to depth scan the film and interface. The low momentum line annihilation lineshape parameter *S* and the high momentum wing parameter *W* were measured at each energy under different substrate temperatures and oxygen partial pressures (0, 4×10^{-3}, 6×10^{-3} and 8×10^{-3} mbar).

Positrons implanted in the sample are thermalized rapidly and then diffuse in the sample. Their implantation profile as a function of the penetration depth z can be described by the Makhovian distribution [19]

$$P(z) = \frac{mz^{m-1}}{z_0^m} \exp\left[-\left(\frac{z}{z_0}\right)^m\right]$$

with

$$z_0 = \frac{\bar{z}}{\Gamma(1+1/m)}$$

where the mean implantation depth $\bar{z}$ is given by

$$\bar{z} = \frac{AE^n}{\rho} \tag{1}$$

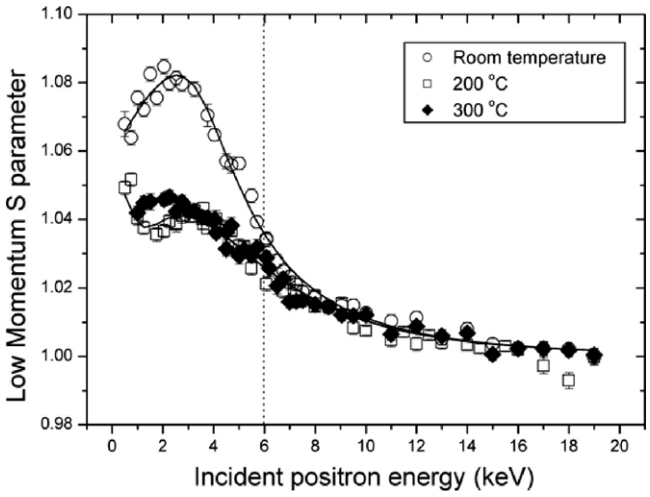

Figure 1. Low momentum *S*-parameter as a function of incident positron energy for ITO/n-GaN fabricated at different substrate temperatures.

where ρ is the density of the sample in g cm^{-3}, E is the implanted positron energy in keV and A, m and n are empirical parameters with values of 4×10^{-6} g cm^{-2}, 2.0 and 1.6, respectively. The lineshape of the annihilation line is first characterized by the 'low momentum' S-parameter which is defined as the ratio of the central region of the 511 keV annihilation photopeak to the total area of the peak. A higher value of the S-parameter thus implies a narrower linewidth and hence more positrons annihilating with low momentum electrons. The W (wing)-parameter, which is also measured, characterizes the higher momentum components of the annihilation lineshape.

The experimental data $S(E)$ were fitted by the computer program VEPFIT [20] which solves the diffusion equation for implanted positrons. The measured S-parameter is a linear combination of the specific S-parameters S_i for different annihilation states in the sample:

$$S = \sum_i f_i S_i \tag{2}$$

where f_i are the fractions of positrons annihilated in the specific states. A similar relationship holds for the W-parameter.

3. Results and discussion

3.1. Variation in growth temperature

Figure 1 shows the variation of the normalized S-parameter with incident positron energy for 100 nm thick ITO films under room temperature and at 200 and 300 °C. In general, one notes a higher S-parameter for low energy implantation falling to the value of the bulk GaN at high energies. Since for implantation energies $E < 6$ keV, the majority of positrons stop in the ITO layer the higher S-parameter observed at energies in this range can be attributed to positron annihilation in the ITO. The S-parameter of the room temperature grown ITO film is thus seen as being significantly higher than the 200 and 300 °C grown films. The remarkable decrease of the S-parameter at higher growth temperatures indicates the film crystallization that occurs when oxygen is incorporated into the ITO lattice at higher temperatures [21, 22]. The room temperature grown film is semi-amorphous with a nanocrystalline structure [23]. The films grown at 200 and 300 °C exhibit much improved crystallinity [24], and thus less open volume, giving an S-parameter which is probably close to that of single crystal ITO. Some

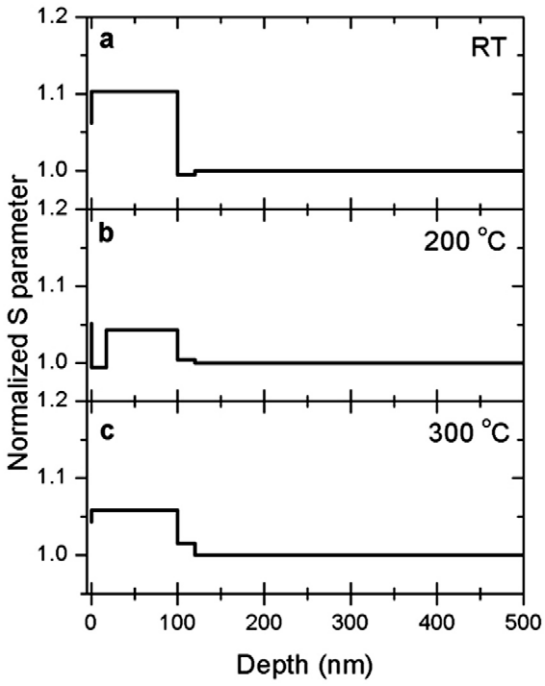

Figure 2. *S*-parameter layer analysis obtained using VEPFIT for ITO/GaN films fabricated at different substrate temperatures.

Table 1. VEPFIT analysis results obtained for the ITO/GaN samples grown under different substrate temperatures.

Sample	Layer number	S_{Li}/S_{GaN}	S_{surf}/S_{GaN}	L_+ (nm)	Thickness (nm)
Sample A, room temperature	1	1.103	1.062	21(1)	100
	2	0.995		1	20
	Bulk	1.000		80	—
Sample B, 200 °C	0	0.994	1.051	14(1)	17
	1	1.043		40 (1)	83
	2	1.004		1	20
	Bulk	1.000		80	—
Sample C, 300 °C	1	1.058	1.043	48(4)	100
	2	1.015		1	20
	Bulk	1.000		80	

caution must be exercised, however, since ITO films are usually polycrystalline or single crystal nanostructures [23, 25, 26] in which case some positron trapping at grain boundaries may also be expected. Habibi *et al* [27] found a mean grain size of 36 nm in ITO film, which with a typical positron diffusion length of ∼100 nm, would indicate a near to saturation trapping at grain boundaries with a positive positron affinity.

Figure 2 shows the results of the VEPFIT analysis of the data. The fitting results are listed in table 1. This modelling is shown by the lines in figure 1. The diagram shows (in histogram form) the *S*-parameters obtained for different block regions assumed for modelling the positron annihilation in the samples. The bulk region for $x > 100$ nm is self-explanatory. Then there is an interface region of thickness 20 nm for which we assume a short positron diffusion length

∼1 nm to model a defect rich positron trapping layer. The third region (0–100 nm) represents the ITO layer. The drop in the *S*-parameter of the ITO film, already commented upon, is now seen more clearly, falling from 1.103 at room temperature to 1.043 and 1.058 at 200 and 300 °C, respectively. The small rise from 200 to 300 °C is possibly due to loss of oxygen from the ITO during deposition. Such a loss would lead to a higher predominance of the defected In_2O_{3-x} phase over the In_2O_3 phase.

The variation of interface *S*-parameter as seen in figure 2 is also revealing. At room temperature, the interfacial *S*-parameter is definitely smaller than that of the GaN bulk. Under 200 and 300 °C growth, it becomes larger. Lower than bulk *S*-parameters are normally associated with the presence of oxygen in the vicinity of defects. The low interfacial *S*-parameter seen in figure 2(a) is thus tentatively attributed to oxygen that has diffused out of the as-deposited ITO and which has either reacted with or has diffused into the GaN. To study the trapping of positrons into ITO oxygen vacancies, the energy band model proposed by Fan and Goodenough [28] is considered. In this model, oxygen vacancies in ITO provide free electrons so that the ITO film becomes degenerate and is most likely becoming metallic in nature. Typical metals, that have an electron concentration of $\sim 10^{22}$ cm^{-3}, have Thomas–Fermi screening lengths given by [29]

$$\lambda_{\mathrm{TF}} = \left(\frac{3\hbar c}{8mc^2\alpha}\right)^{1/2}\left(\frac{\pi}{3n}\right)^{1/6}, \tag{3}$$

where α is the fine structure constant and n is electron density. The screening length in a metal is ∼0.1 nm. For ITO with its slightly lower concentration of $n = 10^{21}$ cm^{-3} this only increases a little to ∼0.14 nm. Thus for ITO as well as metals the electric field produced by any positive centre is negligible outside the defect [30–33]. This is why in metals there is no charge dependent trapping effect as seen in semiconductors. Likewise, in ITO, Thomas–Fermi screening will neutralize the natural positive charge on the V_o^+ defects that have donated carriers, rendering them as positron trapping centres. If the V_o defect is indeed an effective positron trapping site, as suggested, then the decrease in film *S*-parameter at the higher deposition temperatures is most likely to be the result of oxygen incorporation into the ITO as the In_2O_3 and In_2O_{3-x} phases develop.

At the higher deposition temperatures, the *S*-parameter at the interface becomes higher than the bulk, indicating the presence of open volume sites at the interface. Such open volume sites are most likely to be due to the higher lattice mismatch that exists between the GaN and ITO at higher temperature [34]. As mentioned, grain boundaries in the ITO may also trap positrons into regions of lattice mismatch if they have a large enough positron affinity. If this is the case, then the present result would indicate that the open volume sites at the GaN/ITO interface were larger than those found in the ITO film.

The 200 °C grown sample shows an interesting near surface (0–20 nm) feature of low *S*-parameter that is not present in either the room temperature sample or the 300 °C sample. ITO films subject to post-annealing in different gaseous environments show an excess of oxygen at the near surface [16]. The chemical form of this oxygen is known to be different from the In_2O_3 and In_2O_{3-x} phases and its origin is not well understood. One can speculate that at 200 °C oxygen segregates at the surface, while at 300 °C much of this oxygen either incorporates directly into the ITO lattice or is lost from the film as discussed above.

S–*W* plots can be a useful means of detecting the presence of defects in thin films and in distinguishing whether there is just one or more than one defect centre present. Figure 3 shows the *S*–*W* plots for the three growth temperatures where *W* is plotted against *S*. The data have been normalized with the coordinates (1, 1) as the GaN bulk. It is seen that the sample grown at room temperature has data lying on a single line. Even the near surface data lie on the same line.

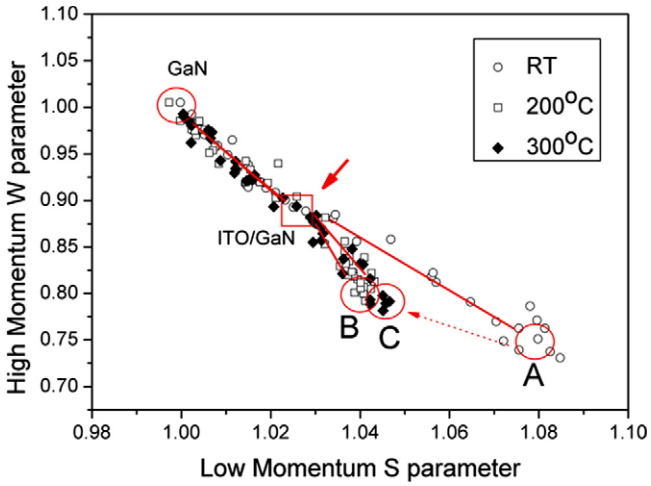

Figure 3. *S*–*W* plot for ITO/GaN films fabricated at different substrate temperatures. The circles show the cluster points associated with the ITO films for (A) room temperature growth, (B) 200 °C growth and (C) 300 °C growth. The square indicates the location of the ITO/GaN.

This demonstrates first the presence of a definitive open volume site in the room temperature grown sample that characterizes the entire film from the near surface through to the interface. These sites are most likely open volumes associated with the nanocrystalline and amorphous structure [16]. The 200 and 300 °C data are remarkably different with the data for both lying on a gradient line that is two segments higher. This difference is due to the crystallization of these films produced during their high temperature growth. The region marked ITO on the plot represents the In_2O_3 phase with some probable mixture of the oxygen deficient In_2O_{3-x} phase. The presence of two segments in the 200 and 300 °C data is caused by defect trapping in the region of the ITO/GaN interface. The square box region shows the *S*, *W* coordinates at the energy that maximizes interface trapping. (It is understood that since there is no single energy at which all the positrons annihilate at the ITO/GaN interface, the *S*, *W* points corresponding to the interface lie somewhere above the GaN/ITO admixture lines.)

3.2. Variation in growth with oxygen partial pressure

Figure 4 shows the *S*-parameter plotted as a function of incident positron energy on the ITO/GaN samples deposited at 200 °C for oxygen partial pressures of 0, 4×10^{-3}, 6×10^{-3} and 8×10^{-3} mbar. In this set of samples a positron implantation energy of ∼10 keV corresponds to the depth of the ITO/GaN interface. Apart from the no-oxygen case the data show a drop in *S*-parameter from a relatively high value (∼1.035) to the GaN value (normalized to be 1.0) at high energies. The high low-energy (<10 keV) value in these samples characterizes the ITO film with some influence coming from the ITO/GaN interface.

The data for growth in the absence of oxygen in figure 4 show a complicated and distinct structure similar to that seen for the 200 °C 100 nm sample deposited. The high value of the *S*-parameter at the ITO/GaN interface indicates that the interface is trapping positrons and has a high concentration of open volume defects. The reduction in the *S*-parameter at low energy (<0.5 keV) indicates a low surface *S*-parameter, while the reduction at ∼6 keV indicates a variation in defect concentration over the ITO film. In general, observers find that ITO films grown with no oxygen overpressure

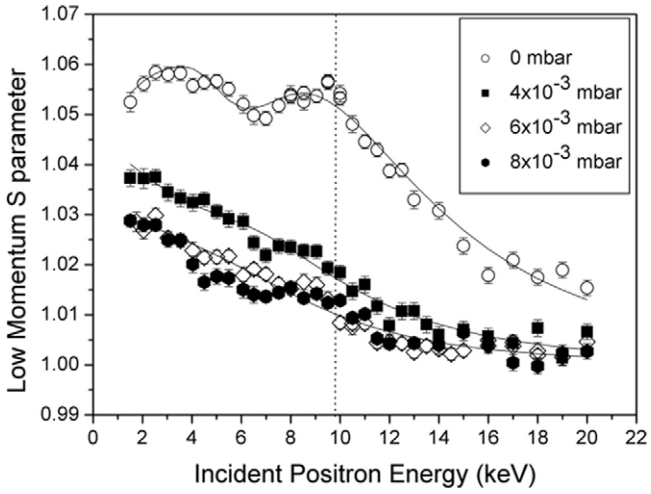

Figure 4. Low momentum *S*-parameter as a function of incident positron energy for ITO/n-GaN fabricated at 200 °C and at different oxygen partial pressures.

are of an amorphous structure with nanocrystals [16]. This being the case, the high *S*-parameter of the ITO film seen here is interpreted as corresponding to open volume sites in the amorphous structure. The significant finding shown in figure 4 is the decrease in *S*-parameter under 2×10^{-3} mbar oxygen partial pressure over the whole implantation energy range; this demonstrates clearly that a higher oxygen partial pressure reduces not only defect trapping at the ITO/GaN interface but also the onset of crystallinity of the ITO film. These results confirm observations made by others that high temperature growth of ITO is not in itself sufficient for good optical and electrical properties, and that oxygenation is necessary for good crystallinity [5, 24]. The results from partial pressures of 2–8×10^{-3} mbar suggest some further reduction in open volume defects indicating further improvements in film crystallinity. However, they also show a definite saturation effect in the oxygenation improvement, with the effect being essentially complete for the 6×10^{-3} and 8×10^{-3} mbar samples.

Figure 5 shows the result of the VEPFIT layer analysis, the fitted curves from which are shown in figure 4. Apart from figure 5(a) (non-oxygenated case) the *S*-parameter data can be fitted with a simple two-layer scheme, the first layer corresponding to the ITO and the second to the GaN bulk. The fitted parameters obtained from VEPFIT are tabulated in table 2. As far as the *S*-parameter analysis is concerned, there is no need to include any interface trapping. The situation in the non-oxygenated case is very different. A high *S*-parameter is required to describe the interface ($S \sim 1.16$). As described above, this indicates large open volume sites at the interface that are able to efficiently trap positrons from both the ITO and the GaN. In addition, the VEPFIT analysis shows that the non-oxygenated ITO film has a definite structure which can be approximated assuming two layers. The first layer, adjacent to the interface, has an *S*-parameter ($\sim$1.03) similar to the oxygenated films, but the near surface layer has a higher *S*-parameter ($\sim$1.06) indicating open volume sites in the ITO film. One explanation for this two-layer structure is that oxygen has segregated at the interface during growth giving rise to quite a good quality film adjacent to the interface. The higher *S*-parameter in the near surface is most likely to be indicative of the amorphous type structure of the ITO film, which only an oxygen overpressure at the surface can prevent from forming. This interpretation is consistent with the non-oxygenated 200 °C growth data (figure 2) taken for the 100 nm thick film, where

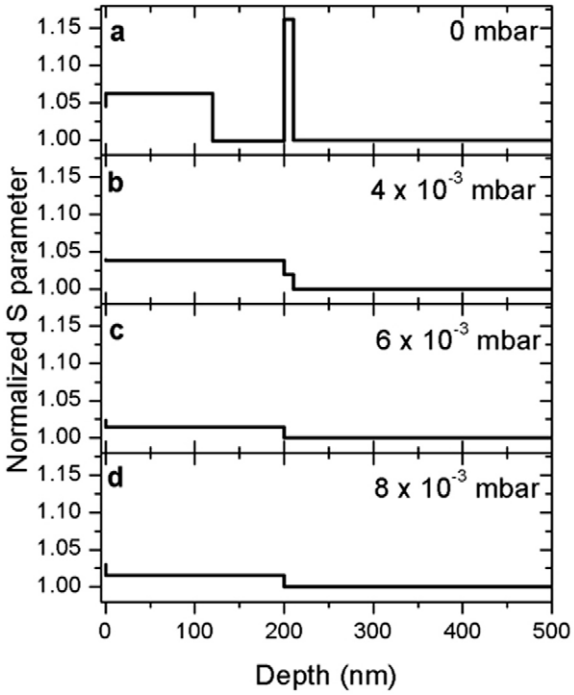

Figure 5. *S*-parameter layer analysis obtained using VEPFIT for ITO/GaN films fabricated at 200 °C and at different oxygen partial pressures.

Table 2. VEPFIT analysis results obtained for the ITO/GaN samples grown under different oxygen partial pressures.

Sample	Layer number	S_{Li}/S_{GaN}	S_{surf}/S_{GaN}	L_+ (nm)	Thickness (nm)
Sample 1,	1	1.062	1.045	16(1)	120
0 mbar	2	1.000		12(1)	80
	3	1.162		3(1)	10
	Bulk	1.000		80	—
Sample 2,	1	1.038	1.039	43(5)	200
4×10^{-3} mbar	2	1.019		10(1)	10
	Bulk	1.000		80	—
Sample 3,	1	1.0146	1.024	136(3)	200
6×10^{-3} mbar	Bulk	1.000		80	—
Sample 4,	1	1.0154	1.030	132(3)	200
8×10^{-3} mbar	Bulk	1.000		80	—

two regions cannot be resolved but where an ITO *S*-parameter value of ∼1.043 is found which lies between the values found for the two layers in the 200 nm case.

The *S*–*W* plot for the oxygenated samples is shown in figure 6. This plot reveals more information than can be obtained from the VEPFIT analysis alone which may be summarized as follows:

(i) For the non-oxygenated sample, the interface can be distinguished as shown by the square cluster point. From this, it can be concluded that the trapping sites at the interface are not

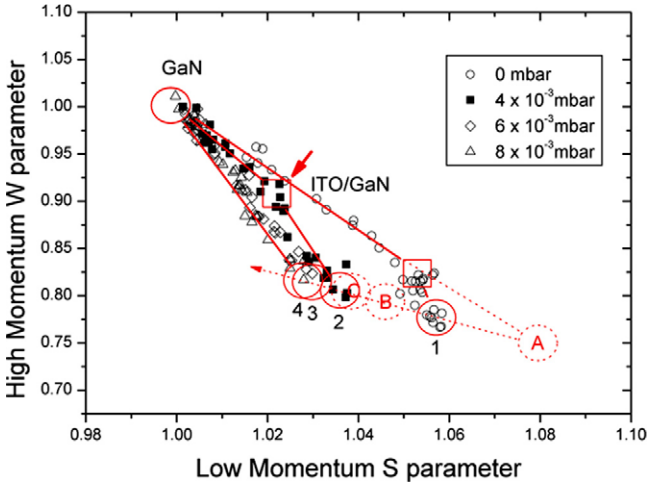

Figure 6. *S*–*W* plot for ITO/GaN films fabricated at 200 °C and at different oxygen partial pressures. The circles show the cluster points associated with the ITO films for (1) 0 mbar, (2) 4×10^{-3} mbar (3) 6×10^{-3} mbar and (4) 8×10^{-3} mbar. The square indicates the location of the ITO/GaN interface.

the same as those in the bulk ITO film. The non-oxygenated data are, however, not of sufficient accuracy to differentiate between the two suggested ITO layers.

(ii) Also shown on the *S*–*W* plot are the ITO film *S*–*W* coordinates (dotted circles) for the 100 nm thick films grown without oxygenation. It is noted that these points lie on the same line as the *S*–*W* coordinates for the oxygenated films. This line is thus indicative of ITO films grown under different oxygen conditions and those films grown with zero oxygen. The fact that there is a single line would suggest that all ITO films only contain a single type of defect and that this defect is just reduced in concentration under a higher oxygen partial pressure. As we have discussed, the oxygen vacancy in the n-type ITO, although expected to be positively charged, will be effectively screened and thus provide a potential positron trapping centre. It thus follows that the defected ITO state displayed in the *S*–*W* plot could simply be the oxygen deficient In_2O_{3-x} phase, in which case the oxygen vacancy would be the most likely candidate for the observed positron trap.

(iii) Only the highly oxygenated (6×10^{-3} and 8×10^{-3} mbar) films show no evidence of an ITO/GaN interface state (the presence of a cluster point at the dashed square). It is concluded that the open volume sites at the interface are removed by oxygenation.

4. Conclusion

ITO films grown using electron-beam evaporation with different substrate temperatures and oxygen partial pressures have been studied using low energy positron implantation. The open volume defect structures in both the ITO film and the ITO/n-GaN interface have been studied using VEPFIT analysis and *S*–*W* plots. The data suggest that there is only one type of defect present in the ITO irrespective of growth conditions, but that the concentration of this defect is reduced with higher temperature growth and under oxygenation. The oxygen vacancy in the In_2O_{3-x} phase is one candidate for the observed positron trap. This observation ties in well with other studies showing that elevated temperatures and threshold levels of oxygen are requisites for ITO films having good electrical and optical properties. At partial pressures of

6×10^{-3} mbar and above we find reduced positron trapping at the ITO/GaN interface indicating better lattice matching. The present study suggests that positron annihilation is an excellent method for characterizing the morphology of ITO films.

Acknowledgments

The work described in this paper is partially supported by the grants from the Research Grant Council of the Hong Kong Special Administrative Region, China (under project no. HKU7021/04P). Financial support from the University Development Fund grant administrated by the University of Hong Kong is also acknowledged.

References

[1] Chang S J, Lee M L, Sheu J K, Lai W C, Su Y K, Chang C S, Kao C J, Chi G C and Tsai J M 2003 *IEEE Electron. Devices Lett.* **24** 212–4
[2] Wang R X, Djurišić A B, Beling C D and Fung S 2005 *Trends in Semiconductor Research* ed T B Ellito (New York: Nova Science) pp 137–74
[3] Kim D W, Sung Y J, Park J W and Yeom G Y 2001 *Thin Solid Films* **398** 87–92
[4] Sheu J K, Su Y K, Chi G C, Jou M J and Chang C M 1998 *Appl. Phys. Lett.* **72** 3317–9
[5] Luis A, De Carvalho C N, Lavareda G, Amaral A, Brogueira P and Godinbho M H 2002 *Vacuum* **64** 475–9
[6] Park S K, Han J I, Kim W K and Kwak M G 2001 *Thin Solid Films* **397** 49–55
[7] George J and Menon C S 2000 *Surf. Coat. Technol.* **132** 45–8
[8] Manivannan P and Subrahmanyam A 1993 *J. Phys. D: Appl. Phys.* **26** 1510–5
[9] Zhang K, Zhu F, Huan C H A and Wee A T 1999 *J. Appl. Phys.* **86** 974–80
[10] Wu W and Chiou B S 1994 *Thin Solid Films* **247** 201–7
[11] Rottmann M, Hennig H, Ziemer B, Kalahna R and Heckner K H 1996 *J. Mater. Sci.* **31** 6465–500
[12] Mori N, Ooki S, Masubuchi N, Tanaka A, Kogoma M and Ito T 2002 *Thin Solid Films* **411** 6
[13] Baia I, Quintela M, Medes L, Nunes P and Martins R 1999 *Thin Solid Films* **337** 171
[14] Huang J L, Jah Y T, Yau B S, Chen C Y and Lu H H 2000 *Thin Solid Films* **370** 33
[15] Tahar R B H, Ban T, Ohya Y and Takahashi Y 1998 *J. Appl. Phys.* **83** 5
[16] Wang R X, Beling C D, Fung S, Djurišić A B, Ling C C and Li S 2005 *J. Appl. Phys.* **97** 033504
[17] Wang R X, Xu S J, Djurišić b_ A B, Beling C D, Cheung C K, Cheung C H, Fung S, Zhao D G, Yang H and Tao X M 2006 *Appl. Phys. Lett.* **89** 033503
[18] Cheung C K, Naik P S, Beling C D, Fung S and Weng H M 2006 *Appl. Surf. Sci.* **252** 3132–7
[19] Makhov A F 1960 *Sov. Phys.—Status Solidi* **2** 1934
[20] van Veen A, Schut H, De Vries J, Hakvoort R A and Ijpma M R 1990 *Positron Beams for Solids and Surfaces* (*AIP Conf. Proc.* vol 218) ed P J Schultz, G R Massoumi and P J Simpson (New York: AIP) p 171
[21] Salehi A 1998 *Thin Solid Films* **324** 214–8
[22] Deng W, Ohgi T, Nejo H and Fujita D 2001 *Appl. Phys.* A **72** 595–601
[23] Ishida T, Kobayashi H and Nakato Y 1993 *J. Appl. Phys.* **73** 4344
[24] Morikawa H and Fujita M 2000 *Thin Solid Films* **359** 61–7
[25] Kulkarni A K, Schulz K H, Lim T S and Khan M 1999 *Thin Solid Films* **345** 273–7
[26] Vink T J, Walrave W, Daams J L C, Baarsky P C and Van Den Meerakker J E A N 1995 *Thin Solid Films* **266** 145–51
[27] Habibi M H and Talebian N 2005 *Acta Chim. Slov.* **52** 53–9
[28] Fan J C C and Goodenough J B 1977 *J. Appl. Phys.* **60** 3524
[29] Blakemore J S 1974 *Solid State Physics* 2nd edn, vol 8 (Philadelphia, PA: Saunders) pp 199–201 (ISBN 0 7216 1701)
[30] Held A and Kahana S 1964 *Can. J. Phys.* **42** 1908
[31] Arponen J and Pajanne E 1979 *Ann. Phys.* **121** 343
[32] Arponen J and Pajanne E 1979 *J. Phys. F: Met. Phys.* **9** 2359
[33] Brandt W 1983 *Positron Solid-State Physics* ed W Brandt and A Pupasquier (Amsterdam: North-Holland) pp 4–8
[34] Shim K H, Paek M C, Lee B T, Kim C and Kang J Y 2001 *Appl. Phys.* A **72** 471